ACS APPLIED MATERIALS & INTERFACES LETTER
www.acsami.org

Lamination of Alumina Membranes to Polymer Surfaces: Thick, Hard, Transparent, Crack-Free Alumina Films on Polymers with Excellent Adhesion

Dalton F. Cheng,[†] Makoto Yagihashi,[‡] and Atsushi Hozumi[*,†]

[†]National Institute for Advanced Industrial Science and Technology, 2266-98 Anagahora, Shimo-Shidami, Moriyama-ku Nagoya, Aichi 463-8560, Japan

[‡]Nagoya Municipal Industrial Research Institute, Rokuban, Atsuta-ku, Nagoya 456-0058, Japan

Supporting Information

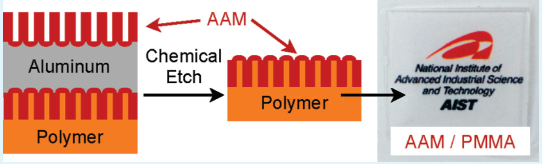

ABSTRACT: Hard and transparent alumina (Al_2O_3) films with thicknesses in the range of 500 nm to 5 μm were successfully formed on polymethylmethacrylate (PMMA) and polystyrene (PS) surfaces. Our process is based on a lamination of anodized aluminum membranes (AAMs) to the polymer surfaces, followed by chemical etching. Because of capillary force, molten PS and liquid PMMA precursor were successfully pulled into the nanopores (10 nm diameter) within the Al_2O_3 layers and solidified by cooling or polymerization, respectively. Our resulting AAM-laminated surfaces exhibited excellent adhesion and surface mechanical properties similar to those of fused silica, remaining crack-free and transparent even with Al_2O_3 thicknesses exceeding 1 μm.

KEYWORDS: anodic oxidation, alumina, alumina membranes, lamination, hard coating, polymer

INTRODUCTION

Thermoplastic polymer materials such as polycarbonate (PC), polymethylmethacrylate (PMMA) and polystyrene (PS) have been widely employed in a wide variety of engineering fields by taking advantage of their excellent properties including light weight, flexibility, transparency, ease of design and coloring, low cost, and good impact resistance. In particular, PC and PMMA have attracted increasing attention lately to be utilized mainly as replacements of glass windows for airplanes, automobiles and buildings.[1] However, because of poor material properties such as scratch resistance and surface hardness, impact and abrasion with harder materials easily disfigures their surfaces, resulting in a decrease in their optical properties. Their low heat resistance also places severe limitations on their surface modifications and treatments. Thus, low temperature formation of hard and transparent layers using UV-curable multifunctional acrylic resins[2] or silicon oxides (SiO_x)[3−10] has been widely demonstrated in industry to improve the mechanical properties of the polymers. However, considering practical usage of such polymeric materials, at present, their mechanical properties, even after surface modification, are insufficient. An alternative hard coating material that can be prepared at low temperature is required for further improvement of their surface mechanical properties. Among the materials that are appropriate for this purpose, metal oxides, i.e., alumina (Al_2O_3) or zirconia (ZrO_2), are particularly promising because of their excellent mechanical and optical properties, and chemical stability. Although many methods including radio frequency plasma,[6,11] chemical vapor deposition,[12] pulsed reactive magnetron sputtering,[13] and pulsed laser deposition[14] for producing such metal oxide films have been reported, significantly high temperatures (generally more than 500 °C) have been typically required to achieve pure and consolidated films. In the case of low-temperature CVD using aluminum acetylacetonate at atmospheric pressure to produce alumina films, the temperature required was still high at 250 °C.[15] In addition, it is common knowledge that the final performance of metal oxide films depends considerably on their thickness. To obtain the best performance (in our case, scratch resistance and hardness), it is frequently required to fabricate a metal oxide film more than 1 μm thick.[16] It would, however, be unfavorable to deposit such a thick oxide film directly on polymeric materials, since the film would crack and/or peel due to the considerable amount of internal stress resulting from the difference between their thermal expansion coefficients. To overcome these problems, an alternative method for metal oxide coatings applicable to polymer substrates, which does not require expensive apparatuses or severe process parameters (precise control of thickness and preparation temperature) has been strongly demanded. For example, a method in which films could be formed with the appropriate material properties on one substrate and transferred to another would be desirable.[17,18]

In this study, we report a novel hard coating technique for polymer substrates using anodic alumina membranes (AAMs) as a hard coating material. It is well-known that amorphous Al_2O_3

Received: May 24, 2011
Accepted: June 21, 2011
Published: June 21, 2011

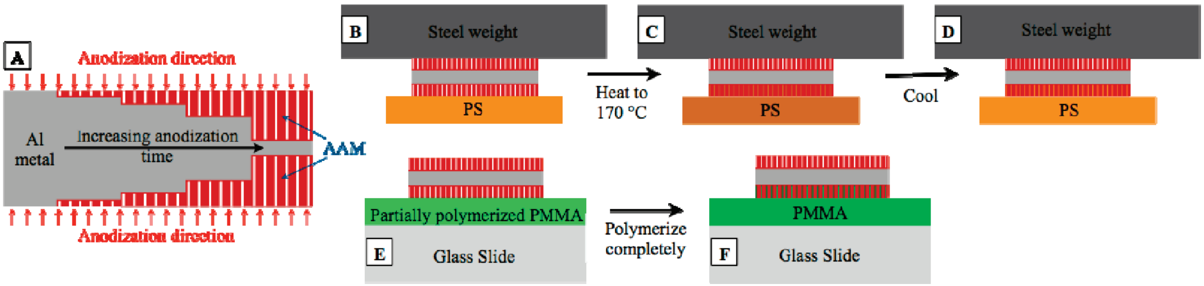

Figure 1. (A) Anodization of Al foil produces pores oriented perpendicularly from the surface. Increasing the anodization time increases the length of the pores. (B) Alumina membranes (AAMs) were placed on bulk PS. (C) The assembly was heated to 170 °C to draw the molten polymer into the pores. (D) Afterward, it was cooled to room temperature. In the case of PMMA, the AAM was placed on a partially polymerized PMMA film (E) to allow capillary forces to draw the viscous liquid into the pores. (F) It was then polymerized completely to produce PMMA nanorods within the AAM pores.

layers with pores oriented perpendicularly from the surface rapidly grow (more than 100 nm/min) on both sides of aluminum (Al) plates at low temperatures during anodic Al oxidation in acidic electrolyte solutions.[19] Their pore sizes, intervals and thicknesses are highly controllable.[20] AAMs have been widely and extensively employed as master molds for the nanofabrication of various kinds of materials.[21,22] The facile release of the rod-like target materials from the nanopores has been investigated to achieve well-ordered nanostructures. For this purpose, surface modifications of the nanopores using functional silanes have been demonstrated.[22] However, there have been no reports on the material use of AAMs as Al_2O_3 hard coatings, in spite of the AAMs offering excellent mechanical and optical properties. Our process demonstrated here has focused on such attractive features of AAMs and consists of only three steps. First, hard, thick and transparent AAMs with various thicknesses were prepared on Al plates through anodic Al oxidation. The pore size was maintained at 10 nm to prevent light diffraction. Next, molten PS or liquid PMMA precursor was inserted into the nanopores through capillary force and solidified by cooling or polymerization, respectively. Finally, the topmost AAM layer and Al support were selectively etched to preserve the remaining Al_2O_3 layer on the polymer surface. The mechanical properties of these AAM-embedded polymers were compared with those of the original polymer and fused silica. Although we only demonstrated the coating of two polymers in this study, i.e., PS and PMMA, our technique has great potential because it enables the formation of various metal oxide layers (besides Al_2O_3), produced through metal anodization, on various types of polymer surfaces with excellent adhesion while preserving their bulk properties without cracking.

RESULTS AND DISCUSSION

Figure 1 shows a schematic illustration of our experimental procedure. First, AAMs with well-ordered nanopores 10 nm in diameter and 45 nm interval were prepared (Figure 1A).[23] By varying anodization time, the thicknesses of the porous oxide layers were precisely controlled, ranging from about 500 nm to over 5 μm. In this study, 4 types of AAMs with different thicknesses (532, 1333, 2666, and 5333 nm) were employed. Out of the two AAMs formed on both sides of the Al foil, one was used as the hard coating layer (the other was removed by chemical etching), whereas the unanodized Al layer served as the mechanical support. In the case of PS (Figure 1B−D), the AAM was placed on a PS sheet. A steel plate served as a weight on top of the AAM to ensure complete contact between the AAM and the polymer surface (Figure 1B). The entire assembly was then heated overnight at 170 °C (Figure 1C), followed by cooling in air to room temperature to resolidify the PS (Figure 1D). On the other hand, in the case of PMMA (Figure 1E,F), after the partially polymerized precursor was spread on a glass slide, an AAM was placed on top of this viscous liquid (Figure 1E), then heated again without weights at 60 °C for 24 h under a dry N_2 atmosphere, resulting in the complete conversion to PMMA (Figure 1F). Finally, the unused AAM and metal Al layers were eliminated step by step through chemical etching (Figure 2).

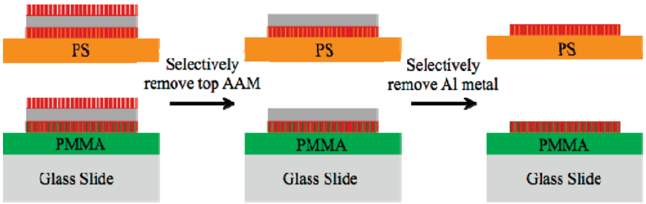

Figure 2. Top-lying AAM and Al metal layers were selectively removed individually to preserve the AAM impregnated with polymer.

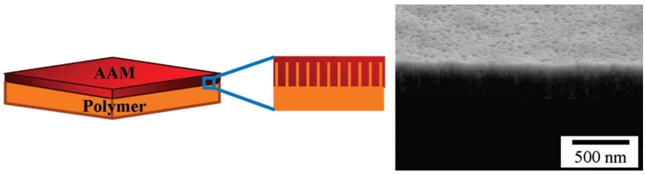

Figure 3. (Left) Image of the AAM/polymer interface. (Right) AAM adhered to PS, viewed from a 30° tilt angle with an SEM. The thickness of the AAM is 532 nm.

After this selective etching, the opposite side of the AAM was exposed toward the air. XPS confirmed that, while there existed tiny impurities of sulfur (3.0 at %) and chlorine (0.8 at %) from the anodization solution and the chemical etchant, respectively, the polymer surface (in this case, PMMA) was undoubtedly covered with a nearly pure Al_2O_3 layer and was completely free of Al metal (see the Supporting Information, Figure S-1). Figure 3 also shows a typical cross-sectional SEM image of the AAM-PMMA interface as a series of polymer nanorods locked within a porous Al_2O_3 matrix. The polymer was expected to have been fully embedded into the AAM nanopores, allowing these two

Table 1. Surface Mechanical Properties of AAM-Laminated PS

AAM thickness	Young's modulus (GPa)	hardness (GPa)
532 nm	24.03 ± 0.89	3.82 ± 0.17
1333 nm	44.99 ± 1.59	4.66 ± 0.22
2666 nm	66.54 ± 1.79	5.85 ± 0.22
5333 nm	78.76 ± 2.78	5.86 ± 0.26
bulk PS only	4.08 ± 0.02	0.26 ± 0.00
fused Silica	74.60 ± 0.57	9.46 ± 0.15

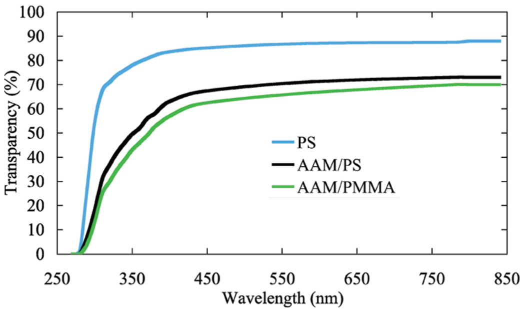

Figure 4. UV–vis spectra of our samples. PS itself has a transparency less than 90%, whereas both AAM-laminated PMMA and PS have transparencies beginning at >70%.

materials to be firmly fixed to one another (see the Supporting Information, Figure S-2).

Because of this AAM lamination, surface mechanical properties (hardness and Young's modulus) of the polymers were completely changed and approached those of fused silica which served as the control sample (Table 1). Although the hardness and Young's modulus of bulk PS is only a few percent of those of fused silica, after the 532 nm thick AAM was laminated to the PS surface, these values increased almost 15 and 6 times, respectively. By using the 1333 nm thick AAM, the resulting surface had a hardness and Young's modulus >50 and >60% that of fused silica, respectively. Finally, for the polymer substrate covered with an AAM over 5 μm thick, the substrate possessed a hardness of almost 6 GPa, >60% that of fused silica, and a Young's modulus that exceeded that of fused silica (74.6 GPa).

Even though the Al_2O_3-polymer interface is tortuous as shown in Figure 3 and the Al_2O_3 surface is bumpy from the anodization process (see the Supporting Information, Figures S-3 and S-4), the resulting sample is nearly transparent. Figure 4 shows a typical example of the UV–vis spectra of PS and PMMA substrates (1 mm thick) covered with 1333 nm thick AAMs and the original PS substrate. It shows good transparency of >70% for the AAM-covered polymer substrates, with the pictures in Figure 5 further demonstrating their clarity and transparency. Even though the AAM was over 1 μm thick, no lamination damage to the layer (e.g., cracking, peeling) was observed as confirmed by optical microscopy (dark-field observation, image not shown). High transparency could be obtained for all samples independent of the polymeric material and AAM thickness, similar to the result shown in Figure 5.

To confirm the adhesive properties of these embedded AAMs on the polymer surfaces, we conducted Scotch tape peeling tests. AAMs on the polymer substrates did not peel off with the tape due to the complete infiltration of the polymers into the nanopores, as described previously. Thus, judging by these results obtained with our technique demonstrated herein, we were able to successfully form Al_2O_3 layers well-adhered to polymer surfaces without using any specific chemical and/or physical surface treatments.

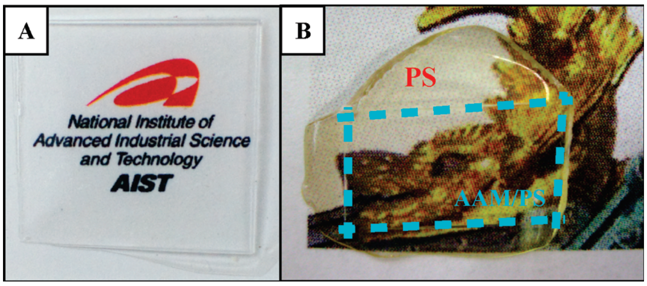

Figure 5. (A) PMMA and (B) PS plates (~1 mm thick) coated with 1333 nm thick AAMs. The transparency on both samples is high and allows for objects behind it (AIST logo for A and Nagoya golden dolphin for B) to be highly visible.

Finally, we further modified the AAM surface with a vapor of D_4^H to produce a hydrophobic surface. The authors have reported previously that chemisorbed D_4^H molecules on a smooth oxidized Al substrate formed a monomeric layer with a thickness of less than 0.5 nm, $\theta_A/\theta_R = 104°/102°$, and 2° contact angle hysteresis.[24] In the present case, a D_4^H-derived monomeric layer is expected to have grown similarly on the AAM surface. The resulting D_4^H-modified AAM-covered polymer surface became highly hydrophobic ($\theta_A/\theta_R = 102°/96°$) with a relatively large contact angle hysteresis (6°). Although our AAM surface is considerably smooth with a R_{rms} of only 1.36 nm, several defects or characteristic bumpy structures may result in a slight increase in contact angle hysteresis (Figure 3 and the Supporting Information, Figures S-3–S-4).

In summary, we have developed a novel hard coating technique for polymer substrates by means of the lamination of anodized aluminum membranes (AAM) to the polymer surface through capillary force, followed by chemical etching. Hard, thick, pure and transparent Al_2O_3 layers with precisely controlled thicknesses of ~500 nm to over 5 μm have been successfully laminated to polymer surfaces with excellent adhesion without cracking, while preserving the optical properties of the original polymeric materials. In contrast to the conventional usage of the AAM as a master mold for the nanofabrication of various target materials reported thus far, our approach is unique and simple and carries great significance.

Our technique, demonstrated here, undoubtedly shows great potential for other metal oxide (not only Al_2O_3) coatings on various polymer substrates (in addition to PS and PMMA) without any marked changes in bulk properties, and may open the path to a wide variety of advanced applications including polymer-made optical components, micromachines, and micro/nanoelectromechanical systems.

EXPERIMENTAL SECTION

Fabrication of AAMs. Aluminum (Al) substrates 1 cm × 2 cm × 250 μm were cut from a mirrorlike Al foil of 99.997% purity (Alfa Aesar, Boston, U.S.A., root-mean-square roughness (R_{rms}) of ~1 nm). They were first electropolished for 20 min at 5 V in a 0 °C solution of 20 vol.% perchloric acid ($HClO_4$) in ethanol.

After electropolishing, the samples were rinsed with Milli-Q water and then dried in air. Next, the samples were anodically oxidized for 2−20 min at 0 °C and 19 V in 2 M sulfuric acid (H_2SO_4). The average thicknesses of achieved Al_2O_3 layers estimated by SEM (JEOL 6320FXV Field Emission Scanning Electron Microscope) were about 532, 1333, 2666, and 5333 nm after 2, 5, 10, and 20 min of anodic oxidation, respectively.

PS and PMMA. In the case of PS, sample substrates 3 cm × 3 cm × 2 mm were cut from a commercial polystyrene (PS) sheet (Asahi KASEI Co., OPS sheet #3000; number-average and weight-average molecular weights were 109 000 and 237 000, respectively). They were rinsed with methanol and then extensively with Milli-Q water to remove impurities. They were then blown dry with a N_2 gas stream. In the case of polymethylmethacrylate (PMMA), a mixture of 99.5 wt % methylmethacrylate and 0.5 wt % 2,2′-azobis(isobutylronitrile) (AIBN) was first polymerized partially at 60 °C for 2 h under nitrogen to increase the viscosity of the liquid and make it easier to form thicker films. By cooling this viscous liquid down to room temperature, polymerization of the precursor could be effectively suppressed.

Selective Etching of Al_2O_3 and Al Layers. In all cases, the exposed Al_2O_3 layer was first etched in an aqueous solution of 10 wt % sodium hydroxide (NaOH) for 20 min. Then the Al metal−support layer was further selectively etched in an aqueous solution (5.9 wt % copper(II) chloride ($CuCl_2$), 19.8 wt % hydrochloric acid (HCl), and 74.3 wt % H_2O) for ∼6 h. Complete elimination of these layers was confirmed by cross-sectional SEM (S-4800, (Hitachi High-Technologies Corp.) and X-ray photoelectron spectroscopy (Quantum 2000 spectrometer, Physical Electronics) using monochromatic AlKα radiation (X-ray source was operated at 50 W and 15 kV).

Characterization. After the chemical etching, the sample was observed by atomic force microscope (AFM, SII: SPA400) using a Si probe (SII, SI-DF20; spring constant = 15 N m^{-1}) with a response frequency of 135 kHz in the tapping mode, and UV−vis spectrophotometer (Hitachi, 340S). Nanoindentation experiments were performed using a Nano Indenter G200 (Agilent Technologies, Inc.) with a Berkovitch-type diamond tip (radius of curvature of 20 nm). From the loading and unloading curves, Young's modulus and hardness were obtained. All data acquired at indentation/displacement of 600−650 nm were determined by averaging values measured at ten different points on each sample surface.

Surface Modification. Samples were modified using a vapor of 1,3,5,7-tetramethylcyclotetrasiloxane (D_4^H) for 72 h at 80 °C based on our previous method.[24] The D_4^H-derived monomeric layer was expected to form on an AAM surface through the formation of Si−O−Al bonds. Changes in surface wettability were monitored by dynamic water contact angles (θ_A and θ_R) measurements (CA-X, Kyowa Interface Science), which were determined using Milli-Q water (10^{18} Ω/cm, ∼3 μL) at room temperature as the water was added and withdrawn from the drop, respectively.

ASSOCIATED CONTENT

Supporting Information. XPS, SEM, AFM, and schematic illustration of the surface of our AAM-laminated polymer surface. This material is available free of charge via the Internet at http://pubs.acs.org.

AUTHOR INFORMATION

Corresponding Author

*E-mail: a.hozumi@aist.go.jp.

ACKNOWLEDGMENT

A.H., M.Y. and D.F.C. thank City Area Program (Development stage) Southern Gifu Area Development of Advanced Medical Equipments By Utilizing Manufacturing and Information Technologies of Ministry of Education, Culture, Sports, Science and Technology (MEXT) for partial support. We also thank Dr. Masaaki Kato of Nagoya Municipal Industrial Research Institute and Dr. Shuichi Asakura of Industrial Technology Center of Gifu Prefectural Government for their technical assistance.

REFERENCES

(1) Hozumi, A.; Takai, O. *Appl. Surf. Sci.* **1996**, *103*, 431–441.

(2) (a) Hozumi, A.; Kato, Y.; Takai, O. *Surf. Coat. Technol.* **1996**, *82*, 16–22. (b) Kushi, K. *Plast. Age* **1985**, *31*, 105.

(3) Mercea, P. V.; Bartan, M. *J. Membr. Sci.* **1991**, *59*, 353–358.

(4) Chatham, H. *Surf. Coat. Technol.* **1996**, *78*, 1–9.

(5) Erlat, A. G.; Spontak, R. J.; Clarke, R. P.; Robinson, T. C.; Haaland, P. D.; Tropsha, Y.; Harvey, N. G.; Vogler, E. A. *J. Phys. Chem. B* **1999**, *103*, 6047–6055.

(6) Rats, D.; Hajek, V.; Martinu, L. *Thin Solid Films* **1999**, *340*, 33–39.

(7) (a) Sobrinho, A. D.; Czeremuszkin, G.; Latreche, M.; Wertheimer, M. R. *Appl. Phys. A: Mater. Sci. Process.* **1999**, *68*, 103–105. (b) Dennler, G.; Houdayer, A.; Latreche, M.; Segui, Y.; Wertheimer, M. R. *Thin Solid Films* **2001**, *382*, 1–3. (c) Dennler, G.; Houdayer, A.; Raynaud, P.; Segui, Y.; Wertheimer, M. R. *Nucl. Instrum. Methods Phys. Res., Sect. B* **2002**, *192*, 420–428.

(8) Zajickova, L.; Bursikova, V.; Perina, V.; Mackova, A.; Subedi, D.; Janca, J. *Surf. Coat. Technol.* **2001**, *142*, 449–454.

(9) Awazu, K.; Onuki, H. *J. Non-Cryst. Solids* **1997**, *215*, 176–181.

(10) Ouyang, M.; Muisener, R. J.; Boulares, A.; Koberstein, J. T. *J. Membr. Sci.* **2000**, *177*, 177–187.

(11) Huang, C.; Yu, Q. S. *J. Appl. Polym. Sci.* **2009**, *116*, 245–251.

(12) Kelekanjeri, V.; Carter, W. B.; Hampikian, J. M. *Thin Solid Films* **2006**, *515*, 1905–1911.

(13) Khanna, A.; Bhat, D. G.; Harris, A.; Beake, B. D. *Surf. Coat. Technol.* **2006**, *201*, 1109–1116.

(14) Hirschauer, B.; Soderholm, S.; Chiaia, G.; Karlsson, U. O. *Thin Solid Films* **1997**, *305*, 243–247.

(15) Maruyama, T.; Arai, S. *Appl. Phys. Lett.* **1992**, *60*, 322–323.

(16) Shirahata, N.; Hozumi, A. *Chem. Mater.* **2005**, *17*, 20–27.

(17) Watanabe, H.; Fujimoto, A.; Takahara, A. *Soft Matter* **2011**, *7*, 1856–1860.

(18) Stafford, C. M.; Harrison, C.; Beers, K. L.; Karim, A.; Amis, E. J.; Vanlandingham, M. R.; Kim, H. C.; Volksen, W.; Miller, R. D.; Simonyi, E. E. *Nat. Mater.* **2004**, *3*, 545–550.

(19) Lee, W.; Ji, R.; Gosele, U.; Nielsch, K. *Nat. Mater.* **2006**, *5*, 741–747.

(20) Li, A. P.; Muller, F.; Birner, A.; Nielsch, K.; Gosele, U. *J. Appl. Phys.* **1998**, *84*, 6023–6026.

(21) (a) Masuda, H.; Satoh, M. *Jpn. J. Appl. Phys. Part 2—Lett.* **1996**, *35*, L126–L129. (b) Sellmyer, D. J.; Zheng, M.; Skomski, R. *J. Phys.: Condens. Matter* **2001**, *13*, R433–R460.

(22) Grimm, S.; Giesa, R.; Sklarek, K.; Langner, A.; Gosele, U.; Schmidt, H. W.; Steinhart, M. *Nano Lett.* **2008**, *8*, 1954–1959.

(23) Kim, B. Y.; Park, S. J.; McCarthy, T. J.; Russell, T. P. *Small* **2007**, *3*, 1869–1872.

(24) Hozumi, A.; Cheng, D. F.; Yagihashi, M. *J. Colloid Interface Sci.* **2011**, *353*, 582–587.